

Fabrication of microcapacitors using conducting polymer microelectrodes

Joo-Hwan Sung, Se-Joon Kim, Kun-Hong Lee*

*Department of Chemical Engineering, Computer & Electrical Engineering Division,
Pohang University of Science and Technology (POSTECH), Pohang 790-784, South Korea*

Received 30 April 2003; accepted 30 May 2003

Abstract

Conducting polymer microcapacitors are fabricated by means of photolithography and electrochemical polymerization techniques. Gold or platinum microelectrode arrays are prepared by UV photolithography and a wet etching method. Conducting polymers such as polypyrrole (PPy) and poly-(3-phenylthiophene) (PPT) are synthesized potentiostatically on these microelectrodes. A microcapacitor is made up of 50 parallel-connected pairs of microelectrodes. The width of the microelectrodes and the distance between them are both 50 μm . Three types of cell are constructed in aqueous and non-aqueous electrolytes, and cell potentials between 0.6 and 1.4 V can be obtained depending upon the type of conducting polymers and electrolytes. Cell capacitance can be controlled easily by the total synthesis charge of the conducting polymers.

© 2003 Elsevier B.V. All rights reserved.

Keywords: Micropower; Electrochemical capacitors; Microcapacitors; Conducting polymers; Photolithography

1. Introduction

Micropower sources have been developed since the 1980s [1]. Thin-film batteries have been the main theme in this field. Developments in micro- and nano-technologies such as microelectromechanical systems (MEMS), nano-electromechanical systems (NEMS), microrobots, and implantable medical devices require micropower sources with smaller dimensions and higher power density. These requirements cannot be satisfied by conventional thin-film batteries as these have lateral dimensions that are greater than 1 cm. Therefore, microscopic power devices have been developed using photolithographic techniques [2,3].

Electrochemical capacitors, also known as supercapacitors, are another type of energy storage device. Generally, their specific energies are greater than those of electrolytic capacitors, and their specific power levels are superior to those of batteries. Thus, the electrochemical properties of supercapacitors are located between those of electrolytic capacitors and batteries. Accordingly, supercapacitors can be used when high power is required and extension of battery discharge time are necessary [4]. If miniaturized to a micron scale, electrochemical capacitors could satisfy a variety of

micropower demands. At present, however, electrochemical microcapacitors are still at an early stage of development [5].

Carbon (active carbon, active carbon fibre and carbon nanotubes), metal oxides (RuO_2 , IrO_2) and conducting polymers (polyaniline (PANi), polypyrrole (PPy), polythiophenes and their derivatives) have been widely used as material for the electrodes of electrochemical capacitors [6–8]. Among these, conducting polymers are attractive materials because they are relatively cheap, autoconductive, and have good specific capacitance ($100\text{--}300 \text{ F g}^{-1}$). Furthermore, they can be synthesized accurately to a sub-micron scale by an electrochemical method. This feature is very advantageous in terms of microdevice fabrication.

Wrighton et al. [9] proposed that conducting polymers could be applied to micropower devices. Following their proposal, we reported the use of conducting polymers such as polypyrrole, polythiophene and their derivatives as electrode materials, together with aqueous or non-aqueous solutions as electrolytes, to make microcapacitors. The devices had power densities that were greater than those of batteries and dimensions of several tens of microns.

2. Experimental

The fabrication procedure for microcapacitors examined in this study is shown in Fig. 1. Gold or platinum microelectrode arrays were fabricated by UV photolithog-

* Corresponding author. Tel.: +82-54-279-2271; fax: +82-54-279-8298.
E-mail address: ce20047@postech.ac.kr (K.-H. Lee).

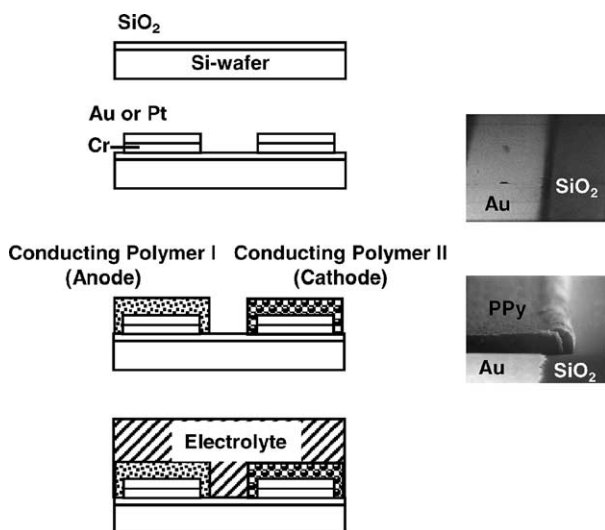


Fig. 1. Fabrication procedure for microcapacitors.

raphy and a wet etching method. Conducting polymers such as polypyrrole and poly-(3-phenylthiophene) (PPT) were potentiostatically synthesized on these microelectrodes. Electrochemical tests were carried out in an aqueous or a non-aqueous electrolyte.

2.1. Fabrication of gold or platinum Pt microelectrode arrays

Gold microelectrode arrays were fabricated on a silicon wafer by means of a photolithographic technique.

Bare Si-wafer ((1 0 0), p-type, LG Siltron Inc.) was oxidized by a wet thermal method to form an insulating layer of SiO_2 with a thickness of 3000 Å. Chromium (200 Å) and gold (500 Å) layers were deposited on the wafer by RF magnetron sputtering. Chromium was used as a buffer layer to enhance the adhesion between gold and SiO_2 . Patterning of gold was carried out with an etching method. A positive photoresist (PR), AZ 5214 (Clariant Corporation), was spin-coated on the gold surface and soft-baked at 90 °C. After UV-exposure through a Cr-Patterned mask, developing was performed using a PR developer, MIF AZ300 (Clariant Corporation) and hard-baking at 120 °C. To remove the exposed gold layer, the wafer was dipped into an aqueous KI/I_2 solution for 30 s, and the exposed chromium layer was removed with a commercial Cr-etchant (CR-7, Cyantek). Finally, residual PR was dissolved in *n*-butyl acetate (Acros Organics).

Platinum microelectrodes were fabricated by the electrodeposition of platinum on gold microelectrodes. The electrodeposition procedure and conditions were identical to a method reported elsewhere [10].

2.2. Electrosynthesis of conducting polymers and electrochemical characterization of microcapacitors

PPy and PPT were synthesized electrochemically on the gold or platinum microelectrode arrays. A three-electrode

arrangement was employed; the working electrode was the gold or platinum microelectrode and the counter electrode was a platinum plate. The reference electrode was Ag/AgCl (saturated KCl) or Ag/0.1 M AgNO_3 (Ag/Ag^+) with corresponding electrolyte medium. All electrochemical experiments were performed with an EG&G model 273 A potentiostat/galvanostat connected to a personal computer. PPy was electrosynthesized on the gold or the platinum microelectrode arrays at 0.65 V versus Ag/AgCl in a 0.1 M pyrrole (Aldrich Chemical Co.,) aqueous solution using 0.1 M KNO_3 (Samchun pure chem.) as a supporting electrolyte at 25 °C, or at 0.5 V versus Ag/Ag⁺ in a 0.1 M pyrrole acetonitrile (ACN) solution using 0.5 M tetraethyl ammoniumtetrafluoroborate (Et_4NBF_4) as a supporting electrolyte (StarLyte, Cheil Ind.) at 18 °C until desired charges were reached. After synthesis, the PPy electrodes were kept in a doped state as-prepared because PPy in this state is stable in air. PPT was also potentiostatically polymerized on Pt electrodes at 0.98 V versus Ag/Ag⁺ in a 0.09 M 3-phenylthiophene (Tokyo, Kasei) ACN solution using 1.0 M Et_4NBF_4 as a supporting electrolyte at 25 °C. After synthesis, PPT electrodes were de-doped at -0.4 V until the de-doping current fell below 1 μA because of its high environmental stability when it is de-doped [11]. Tests on full cells were performed in a beaker-type electrochemical cell where only the electroactive part was dipped in the electrolyte solution. Prior to all experiments, dry N_2 was bubbled through the electrolyte solutions for 30 min, and all electrochemical tests were performed in a dry nitrogen atmosphere. All reagents were used without further purification.

3. Results and discussions

Gold microelectrode arrays were fabricated by the photolithographic technique, which can accurately control the electrode size, the distance between the anode and the cathode, and the geometry from several tens of millimeters to a sub-micron scale. The width of an electrode and the distance between two electrodes were both 50 μm . The geometry was a comb-like structure, as shown in Fig. 2. The prototype had 50 pairs of microelectrodes, to give a parallel connection of 50 microcapacitors. Three types of microcapacitor cell were constructed, depending on the type of conducting polymers and electrolytes. The construction and characteristics of each cell are summarized in Table 1.

Scanning electron microscopic (SEM) images of two types of microcapacitor are shown in Fig. 3. The N1 cell is made up of PPy electrodes with capacities and thicknesses that are almost the same. Electron micrographs were obtained after PPy electrodes were doped with BF_4^- and dried. The electrodes are granular in shape and densely packed at the edge of the current-collectors. At the edge position, the electric field is enhanced, and so the PPy electrodes are more easily electrosynthesized than on the flat surface. The N2 cell is composed of PPy and the PPT

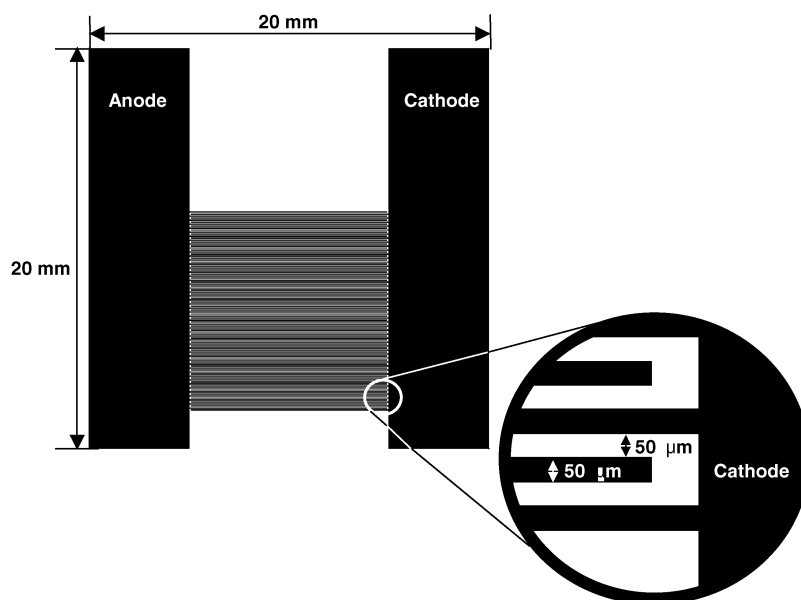


Fig. 2. Schematic configuration of microcapacitors.

microelectrodes. In this configuration, Pt microelectrodes are used as the current-collectors. The PPT electrodes are also granular in shape and densely packed at the edges of the current-collectors. PPT electrodes were indistinguishable from PPy electrodes at a low resolution. The size of the PPT granules is smaller than that of the PPy granules at a high resolution (not shown). As PPy and PPT have higher vertical growth rates than lateral ones, the thickness can be controlled by the synthesis charge.

3.1. Electrochemical tests in aqueous media

To fabricate microcapacitors that can be operated in aqueous electrolytes, PPy and polyaniline were selected as the electrode materials because they are electropolymerizable and electroactive in aqueous media. In the case of PANi, however, adjacent electrodes were interconnected during synthesis due to the high lateral growth rate of PANi. It is assumed that the high affinity between the aniline monomer and the SiO₂ substrate causes preferential growth in the lateral direction [12]. On the other hand, PPy is adequate for this application because PPy had higher vertical growth rates.

In order to assure uniform electrosynthesis throughout all the gold microelectrodes, the electrosynthesis of conducting polymers was performed potentiostatically, because galvanostatic electropolymerization results in non-uniform film thickness over the entire cell. To make the cathode and the anode electrochemically identical, two PPy electrodes were synthesized simultaneously. Cyclic voltammograms for PPy–PPy microcapacitors in aqueous solution containing 0.1 M H₃PO₄ (Al cell) are shown in Fig. 4. All the microcapacitor cell display capacitive behaviour. As the synthesis charge is proportional to the amount of PPy synthesized, the greater the charge used for PPy synthesis, the larger is the capacitive current.

The capacitive current does not, however, show a linear correlation with synthesis charge. For PPy electrodes, it has been reported [13] that the currents are smaller than those calculated by the linear correlation above 1 μm thickness. Moreover, the thicker film does not show typical capacitive behaviour, but a little non-flat behaviour, which may be due to a decrease in ionic conductivity. It is known that an increase in film thickness lowers the ionic conductivity inside a conducting polymer film, and hence the electrochemical behaviour deviates from ideal because

Table 1
Construction and characteristics of microcapacitor cells

Cell	Electrode		Electrolyte	Cell potential (V)	Capacitance (mF) ^a	R _b (Ω) ^b
	Anode	Cathode				
A1	PPy	PPy	0.1 M H ₃ PO ₄ (aq.)	0.6	1.6–14	6.3–7
N1	PPy	PPy	0.5 M Et ₄ NBF ₄ (ACN)	0.8	3.9	4
N2	PPy	PPT	0.5 M Et ₄ NBF ₄ (ACN)	1.4	5.2	3.9

^a Cell capacitance at 5 mHz from impedance spectroscopy.

^b R_b (solution resistance) calculated from impedance spectroscopy.

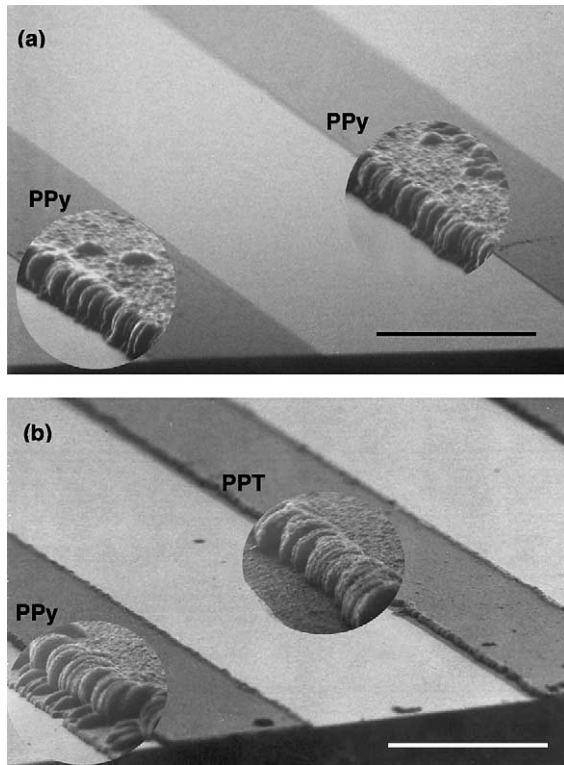


Fig. 3. Electron micrographs of (a) N1 and (b) N2 microcapacitor electrodes. PPy (a) synthesized on gold microelectrodes, and PPy and PPT (b) on platinum microelectrodes. All conducting polymers are doped with BF_4^- ions.

the doping–de-doping of conducting polymers is a bulk reaction.

For each A1 cell, impedance spectroscopy experiments were carried out at the open-circuit potential. Frequency dispersions of capacitance for each cell are shown in Fig. 5a and c. Capacitance (C_f , mF) and relative capacitance (C_{rel}) were calculated from the following equations:

$$C_f = \frac{1}{2\pi f Z_{\text{im}}} \quad (1)$$

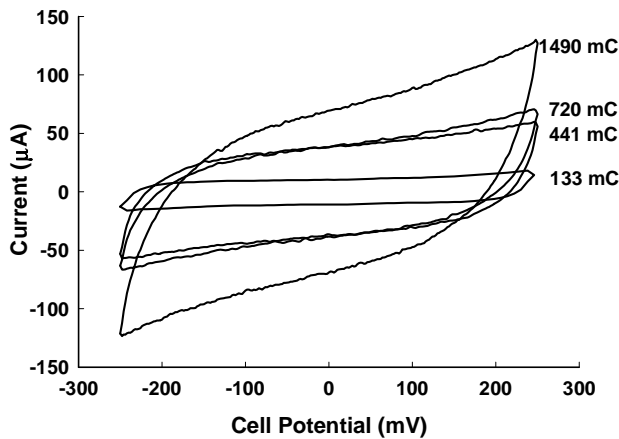


Fig. 4. Cyclic voltammograms for A1 microcapacitors in aqueous 0.1 M H_3PO_4 . Charge represents total charge used for PPy synthesis scan rate is 10 mV s^{-1} .

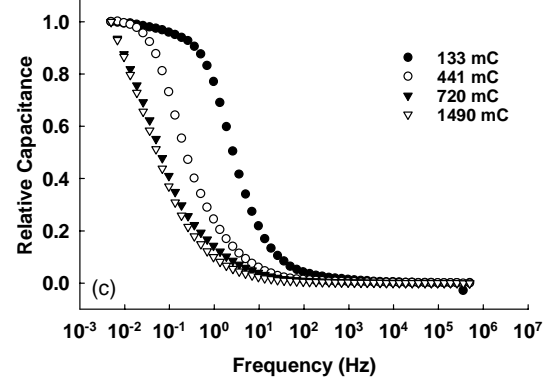
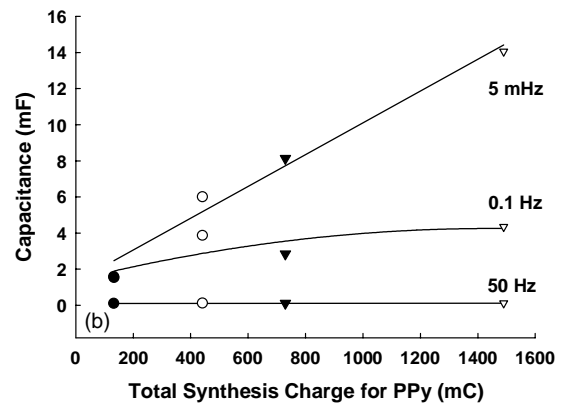
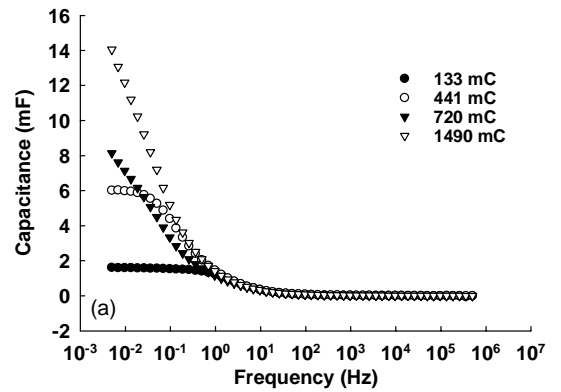


Fig. 5. (a) Frequency dispersion of capacitances, (b) relationship between total charge used for PPy synthesis and capacitance obtained at 5 mHz, (c) frequency dispersion of relative capacitances for A1 microcapacitors. Impedance spectroscopies conducted at open-circuit voltage with ac amplitude of 5 mV rms.

$$C_{\text{rel}} = \frac{C_f}{C_{5 \text{ mHz}}} \quad (2)$$

where f is the frequency, Z_{im} the imaginary part of impedance, and $C_{5 \text{ mHz}}$ is the capacitance at 5 mHz. By varying the thickness of PPy films, the electrochemical behaviour of microcapacitor could be controlled. When the amount of PPy increases, the capacitance of a microcapacitor increases though the increase is restricted to a limited frequency region. At very low frequencies ($f < 0.01 \text{ Hz}$), a linear relationship between the film thickness and capacitance is observed. At moderate frequencies ($0.01 \text{ Hz} <$

$f < 1$ Hz), however, the capacitance cannot be correlated with the amount of PPy. On increasing the frequency to a very high value, capacitances are very low and similar irrespective of the film thickness (Fig. 5a and b). From the frequency dispersion of relative capacitances shown in Fig. 5c, the effect of thickness on the electrochemical behaviour of PPy films can be investigated more efficiently. The capacitances decrease dramatically with increase in frequency at a much lower frequency range for thick PPy films, while the capacitances are stable to relatively higher frequencies for thin films. Given that the microcapacitor cells are identical in the distance between electrodes, the electrolyte and the cell resistance, but differ in the thickness of the PPy films, the electrochemical behaviour may result from the difference in the ionic conductance through the films. As the film thickness increases, the ionic mobility through the film decreases; therefore, these retarded ions are unable to keep pace with rapid changes in frequency.

The discharge performance of an A1 cell at currents between 0.001 and 0.5 mA is shown in Fig. 6. Intrinsically conducting polymers show pseudocapacitive behaviour. Pseudocapacitance arises when the charge q , required for an electrode reaction is a continuous function of potential V [14]. Because of charge continuity, the potential decreases. On the other hand, the potential in batteries is relatively constant during discharge. This difference in characteristics distinguishes batteries from electrochemical capacitors. The IR drop of the cell is negligible, irrespective of the

discharge rate due to the narrow anode to cathode distance ($< 50 \mu\text{m}$) and the absence of a separator. In particular, as a separator may give rise to high cell resistance, the structure of a cell which contains no separator could enhance the electrodynamic properties.

Cyclic voltammograms for the cathode and the anode in the above cell are also shown in Fig. 6. Because both electrodes were prepared simultaneously, their synthesis conditions were identical. The voltammograms are very similar; polymer degradation (> 0.3 V) and hydrogen evolution (< -0.4 V) restrict the stable potential region to only 0.6 V.

3.2. Electrochemical tests in non-aqueous media

Water is a good solvent because it is abundant and its solvent properties are attractive in many applications. Nevertheless, water is losing popularity in energy devices, due to its corrosiveness and a narrow potential window. In organic electrodes based on conducting polymers, a small amount of water might react with the organic materials and deactivate the electrochemical properties when the applied potential is high [15]. If aqueous electrolytes are used for conducting polymer electrodes, the practical potential window may become narrower than its usual potential window (1.23 V). Therefore, non-aqueous solvents play major roles in batteries and electrochemical capacitors. By adopting such solvents, various conducting polymers such as polythiophene and its derivatives which have operating potentials that are

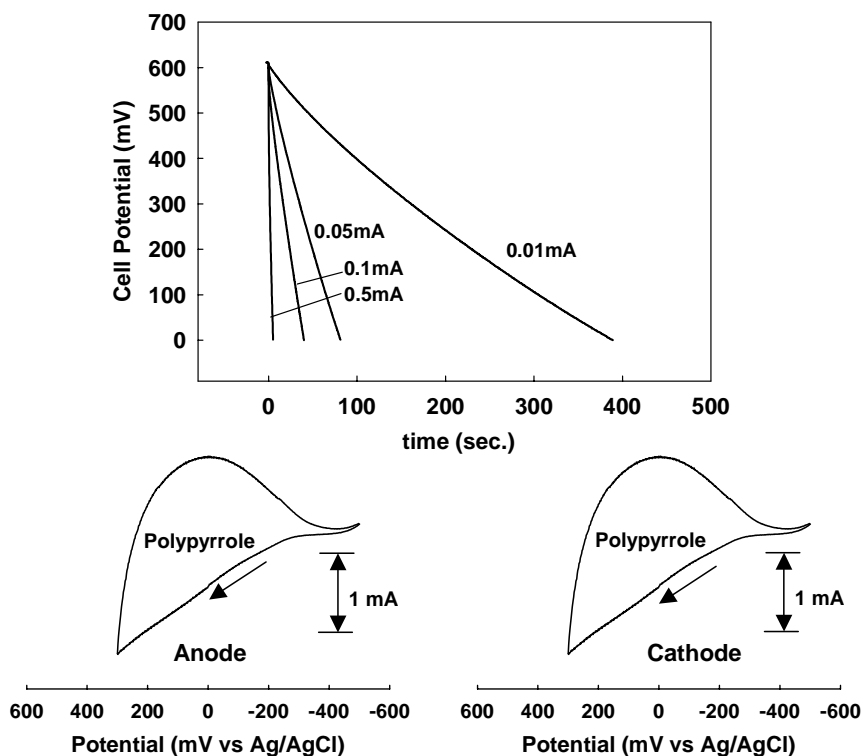


Fig. 6. Constant-current discharge of A1 microcapacitors, and cyclic voltammograms for cathode and anode in an aqueous 0.1 M H_3PO_4 (scan rate: 50 mV s^{-1}).

much higher than other conducting polymers, can be applied to microcapacitor systems. Because conducting polymers synthesized in aqueous solutions are not electroactive in non-aqueous media, in this study all conducting polymers have been synthesized in non-aqueous acetonitrile solutions which contain Et_4NBF_4 solutes.

Cyclic voltammograms of PPy electrodes in ACN are different to those obtained in aqueous solutions (Fig. 7). The types of solvent and solute have decisive effects on the electrochemical behaviour of conducting polymers. Therefore, different peak positions and current densities can be obtained for the same polymers, as dictated by the type of electrolyte solution. As reported in Table 1, PPy–PPy microcapacitors operated in non-aqueous media (N1 cell) have higher cell potentials (~ 0.8 V) than in aqueous electrolytes.

The absence of H^+ ions and the wide potential window of the Et_4NBF_4 –ACN solution enables PPy–PPy microcapacitors to operate at higher potentials. The discharge behaviour is similar to that of the A1 cell, except for a fast initial decay. The difference in initial performance will be discussed later.

The specific energy of an electrochemical capacitor can be calculated from the relationship $E = 1/2CV^2$, where C is the capacitance and V is the potential. Clearly, the latter parameter is the most important factor that determines the specific energy, because the amount of energy is proportional to V^2 . By choosing different conducting polymers which have different potential ranges, microcapacitors can be designed with higher or lower cell potentials. If p-dopable conducting polymers are used as an anode as well as a cathode, low

cell potentials (< 1.0 V) can be obtained. By contrast, higher cell potentials can be obtained with electrodes that differ in the conducting polymer chosen. As the potential range of PPT is more positive, it is possible to construct a complete cell by using PPy as the anode and PPT as the cathode (N2 cell). Furthermore, potential overlapping is small for this pair. The constant-current discharge of the N2 cell is shown in Fig. 8. It is impossible for this cell construction to be used in an aqueous medium due to the corrosion of PPT by water molecules. It has been found that the electrochemical current of PPT decays rapidly on cycling with a small amount of water. The PPTs were electrosynthesized on platinum microelectrodes, because gold electrodes became corroded at the high synthesis potential of PPT (0.98 V versus Ag/Ag^+). By using a PPy–PPT pair, a cell voltage of 1.4 V could be obtained. Rapid decay regions in cell voltage were observed during the initial discharge stage, and the final voltage was 0.8 V. A similar initial rapid decay of voltage was also shown by the N1 cell. In order to investigate this phenomenon, constant-current discharge was performed separately for each electrode. An initial decay in discharge behaviour is displayed by PPy, but a final decay by the PPT electrode (Fig. 9). These effects can be explained by examination of the cyclic voltammograms for PPy and PPT electrodes (Fig. 8). It is seen that PPy gives an anodic current only above -0.5 V and a cathodic current above -0.7 V. Thus, if PPy electrodes are used as anodes, the anodic current response is the discharge current and the cathodic current is the charge current. Although such-electrodes can

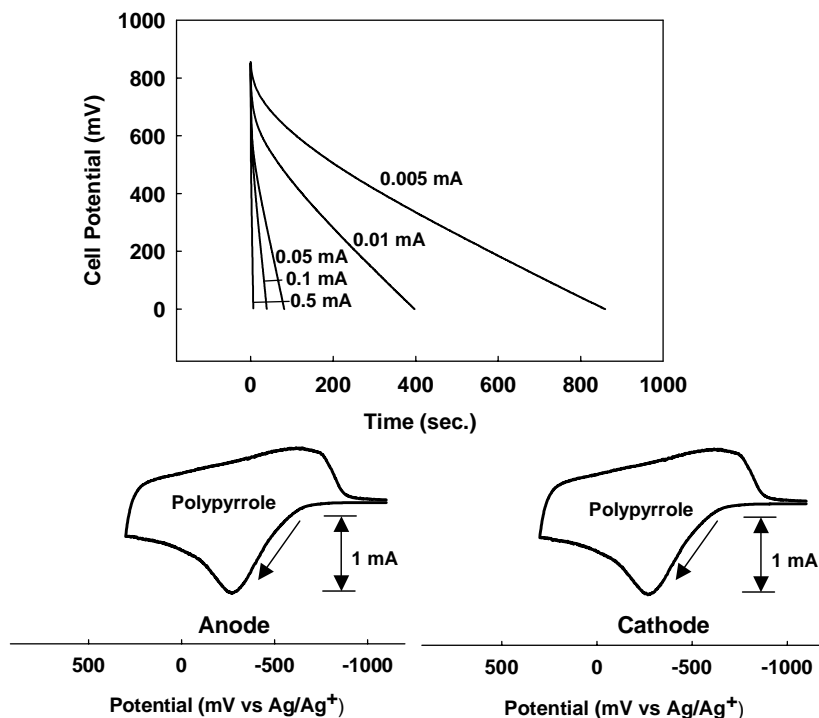


Fig. 7. Constant-current discharge of N1 microcapacitors, and cyclic voltammograms for cathode and anode in 0.5 M Et_4NBF_4 –ACN solution (scan rate: 50 mV s^{-1}).

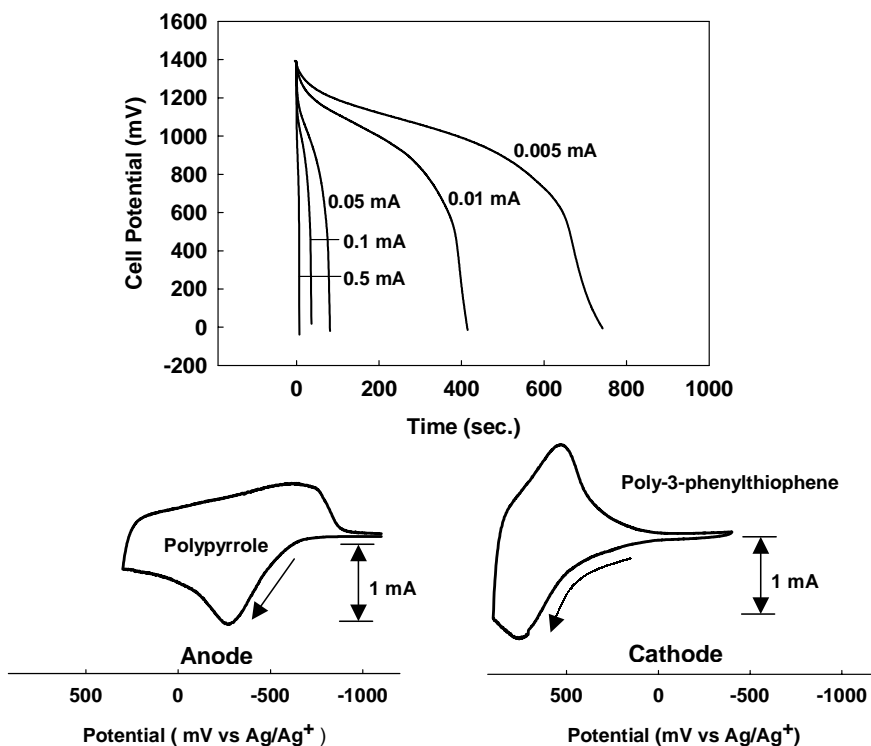


Fig. 8. Constant-current discharge of N2 microcapacitors, and cyclic voltammograms of the cathode and the anode in a 0.5 M $\text{Et}_4\text{NBF}_4\text{-ACN}$ solution (scan rate: 50 mV s^{-1}).

be charged below -0.7 V , it is discharged from -0.5 V . Therefore, the charging potential and the starting potential of discharge may have different values, and this will cause an initial potential decay on discharge. On the other hand, the charging and discharging potentials of PPT are the same, as shown in the cyclic voltammogram for PPT in Fig. 8. As PPT is used as the cathode in the above cell design, the cathodic current is the discharge current. Since cathodic current exists only above 0.2 V , the potential of the PPT electrode under constant-current discharge rapidly decays from 0.2 V . If a conducting polymer with a potential which sufficiently overlaps that of PPY is used, the rapid decay at

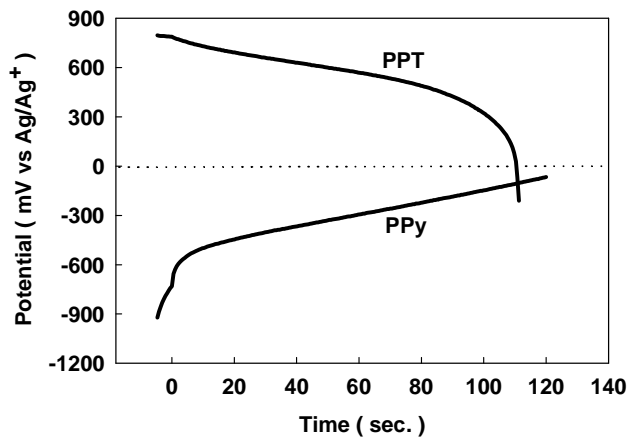


Fig. 9. Constant-current discharge of PPY and PPT microelectrodes in $0.5 \text{ M Et}_4\text{NBF}_4\text{-ACN}$ solution. Discharge current: 0.05 mA .

low cell voltage will be diminished, though the maximum cell potential will be lowered. The selection of conducting polymers depends on the purpose of the application.

Nyquist plots of PPY–PPY cell constructions are presented in Fig. 10. The impedance behaviour is very different and is determined by the thicknesses of PPY electrodes and the electrolytes. The solution resistance, R_b , which is the intercept with the real axis in the high-frequency region, has a value of a few ohms. For aqueous electrolytes, the numerical values of R_b are about the same, irrespective of the film thicknesses. In the case of $0.5 \text{ M Et}_4\text{NBF}_4\text{-ACN}$ electrolytes, however, R_b is much smaller due to its larger ionic conductivity (aqueous $0.1 \text{ M H}_3\text{PO}_4$ solutions: $\sim 11 \text{ mS m}^{-1}$; $0.5 \text{ M Et}_4\text{NBF}_4\text{-ACN}$ solutions: $\sim 18 \text{ mS m}^{-1}$). The ratio of the conductivities of the two electrolytes is almost equal to that of R_b . Since the distance between the electrodes and the cell geometry are exactly the same, the difference in R_b originates solely from the electrolytes.

In summary, three types of microcapacitor with different electrode materials and electrolytes have been reported. Cell geometry such as the distance between microelectrodes, number and size of the microelectrodes, thickness of the conducting polymer and cell capacity can be controlled accurately by photolithography and electrochemical synthesis of the conducting polymers. Microcapacitors with various capacities and voltages can be easily fabricated by designing corresponding photomask patterns. Selection of the electrode materials and electrolytes is a decisive factor for the cell properties. Although the microelectrodes reported

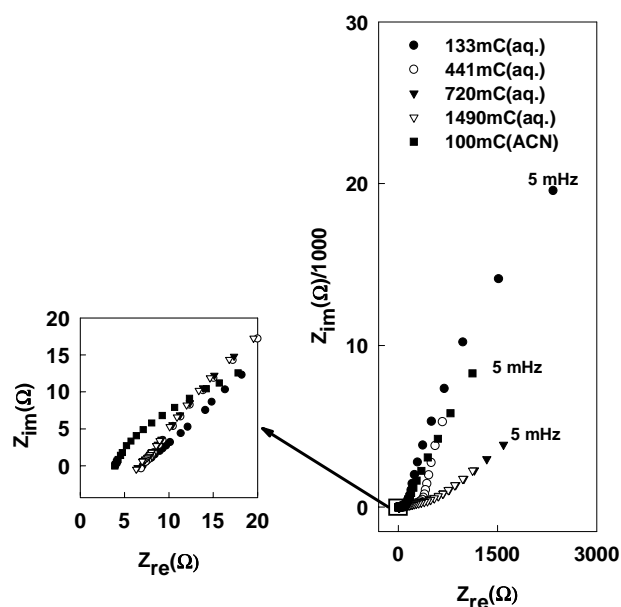


Fig. 10. Nyquist plots of PPy-PPy microcapacitors in different electrolytes. Impedance spectroscopies conducted in aqueous 0.1 M H_3PO_4 and 0.5 M Et_4NBF_4 -ACN charge numbers represent total charge used for PPy synthesis.

here have been made on the scale of several tens of microns in order to simplify fabrication and electrochemical analysis, microelectrodes with sub-micron dimensions are possible if corresponding gold or platinum microelectrodes are available. Microcapacitors with solid electrolytes, which have no leaks and are thus easy to fabricate, can be incorporated into various MEMS devices and microrobots. Such devices are under investigation in the authors laboratory.

Acknowledgements

This work was supported by the POSRIP and by the BK21 program of the Ministry of Education of Korea.

References

- [1] K. Kanehori, K. Matsumoto, K. Miyauchi, T. Kudo, *Solid State Ionics* 9–10 (1983) 1445.
- [2] K. Kinoshita, X. Song, J. Kim, M. Inaba, J. Power Sources 81–82 (1999) 170.
- [3] L.G. Salmon, R.A. Barksdale, B.R. Beachem, R.M. Lafollette, J.N. Harb, J.D. Holladay, P.H. Humble, *Solid-State Sensor and Actuator Workshop Proceedings*, 1998, p. 338.
- [4] B.E. Conway, *Electrochemical Supercapacitors*, Kluwer Academic/Plenum Publishers, New York, USA, 1999, pp. 1–31.
- [5] J.H. Lim, D.J. Choi, H.K. Kim, W.I. Cho, Y.S. Yoon, *J. Electrochem. Soc.* 148 (2001) A275.
- [6] J.P. Zheng, J. Huang, T.R. Jow, *J. Electrochem. Soc.* 144 (1997) 2026.
- [7] J.P. Zheng, T.R. Jow, *J. Electrochem. Soc.* 142 (1995) 2699.
- [8] S. Panero, E. Spila, B. Scrosati, *J. Electroanal. Chem.* 396 (1995) 385.
- [9] M.S. Wrighton, H.S. White Jr., J.W. Thackeray, US Patent 4,717,673 (1988).
- [10] C. Haro, R. Mas, G. Abadal, J. Muñoz, F. Ferez-Murano, C. Dominguez, *Biomaterials* 23 (2002) 4515.
- [11] H.S. Nalwa, *Handbook of Organic Conductive Molecules and Polymers*, vol. 3, Wiley, New York, USA, 1997, pp. 795–856.
- [12] M. Nishizawa, M. Shibuya, T. Sawaguchi, T. Matsue, I. Uchida, *J. Phys. Chem.* 95 (1991) 9042.
- [13] B. Zinger, L.L. Miller, *J. Am. Chem. Soc.* 106 (1984) 6861.
- [14] B.E. Conway, V. Birss, J. Wojtowicz, *J. Power Sources* 66 (1997) 1.
- [15] K. Izutsu, *Electrochemistry in Nonaqueous Solutions*, Wiley/VCH, Weinheim, Germany, 2002.